

# Joint Rate and Power Adaptation for Type-I Hybrid ARQ Systems Over Correlated Fading Channels Under Different Buffer-Cost Constraints

Dejan V. Djonin, Ashok K. Karmokar, *Student Member, IEEE*, and Vijay K. Bhargava, *Fellow, IEEE*

**Abstract**—We present a general framework for the computation of the optimal scheduling policies for delay and overflow-constrained joint rate and power adaptations for type-I hybrid automatic-repeat-request systems. This framework can be applied to adaptive resource-allocation problems on correlated flat-fading or frequency-selective fading channels for bursty nonconstant packet arrivals. It is shown that the optimal-rate and power-control laws can be obtained by solving the formulated Markov decision process problems. We consider two cases for packet scheduling over wireless channels that are of significant practical importance. In the first case, we assume that the transmitter perfectly knows the channel-state information (CSI) at the beginning of the transmission. The transmitter is also provided with the decoding result for the previous transmission in terms of observation feedback at the end of the transmission. Second, we consider the scheduling problem when the transmitter does not know the CSI at the time of transmission, but it makes the transmission decision based on the history of previous transmissions and corresponding outcomes. In both cases, our objective is to minimize transmission power, and the optimal policies are computed under two different buffer-cost constraints, namely, the average buffer delay and the average packet overflow rate. The results of this paper are of importance for the development of modern wireless standards that support heterogeneous multimedia and Internet traffic with certain application-dependent-delay and packet-dropping requirements.

**Index Terms**—Adaptive type-I hybrid automatic repeat request (ARQ), finite-state Markov channel (FSMC), joint transmission rate and power adaptation, Markov decision process (MDP), non-constant bursty traffic, packet scheduling, partial channel-state information (CSI).

## I. INTRODUCTION

**A**DAPTIVE resource-allocation schemes have been proven to be a useful means of increasing the capacity and the reliability of wireless transmission links. The main idea behind these schemes is the adaptation of some of the parameters

Manuscript received March 8, 2004; revised November 29, 2005, July 26, 2006, and February 17, 2007. This work was supported in part by the Natural Sciences and Engineering Research Council (NSERC) of Canada under a strategic project grant, by the University of British Columbia Graduate Fellowship Award, and by the NSERC Postdoctoral Fellowship Award. This paper was presented in part at the IEEE Global Telecommunications Conference (GLOBECOM 2004), Dallas, TX, November 29–December 3, 2004. The review of this paper was coordinated by Prof. H. Leib.

D. V. Djonin is with Dyaptive Inc., Vancouver, BC V6E 3C9, Canada (e-mail: ddjonin@ece.ubc.ca).

A. K. Karmokar and V. K. Bhargava are with the Department of Electrical and Computer Engineering, University of British Columbia, Vancouver, BC V6T 1Z4, Canada (e-mail: ashokk@ece.ubc.ca; vijayb@ece.ubc.ca).

Digital Object Identifier 10.1109/TVT.2007.901876

(e.g., transmitter power level, modulation scheme, coding rate, etc.) of the transmitter based on the information of the channel conditions [sometimes also called the channel-state information (CSI)] of the wireless fading channel [1], [2]. These systems, in general, require some form of channel estimation either at the transmitter or at the receiver. The estimated information of the channel at the receiver is sent over a feedback channel. Adaptive resource allocation has already found its practical application. It has been provisioned for several wireless standards such as EDGE, third-generation (3G) evolution standards 1xEVDO, etc. Furthermore, next-generation wireless networks are envisaged to support high data rates, packet-oriented transport, multimedia traffic, and wide range of quality-of-service (QoS) requirements [e.g., delay, bit error rate (BER), packet-loss probability, etc]. In this paper, we have presented an approach to optimize these goals across the physical and data-link layers. The problem of power and rate adaptations has first been analyzed from an information-theoretic viewpoint (e.g., in [3]), where optimal water-filling power control law that maximizes the ergodic capacity of a time-varying channel is derived. More practically oriented results have been given in [4] that analyzes rate and power adaptation for  $M$ -QAM systems. This line of research has been further extended in [2], where different optimization criteria and different resource adaptation techniques have been compared. The adaptive modulation schemes proposed in [2] and [4] choose the modulation constellation based only on the channel condition. Assuming an infinite transmitter buffer, the aforementioned conventional adaptive modulation scheme does not consider the buffering delay and the packet loss due to overflows. These schemes also have not considered the packet-arrival statistics and have assumed that packets are always available for transmission in the buffer.

From a higher layer perspective, resource adaptation techniques for time-varying fading channels, in general, require the use of a finite transmission buffer to provide a degree of flexibility in handling the time-varying number of transmitted packets. This buffer introduces time-varying delay in the transmission of packets, which can have detrimental effects on the transmission of delay-sensitive data such as voice or video traffic over wireless channels. The effect of the delay variation is even more exacerbated in the case of slow-fading channels where long deep fades can introduce intolerable delays in transmission. Buffer overflow is another important factor that should be taken into consideration while considering communications

of finite buffer systems over slow-fading channels. Cross-layer optimization has recently attracted the attention of wireless research community. It has been shown that adapting system parameters across different open-system interconnection (OSI) system layers can significantly improve the system performance [5]. An early work of Collins and Cruz [6] gives a dynamic programming framework for transmission policies over a simple two-state channel with a constraint on average delay and peak power. Offline and online packet-scheduling schemes for an additive Gaussian noise channel have been analyzed in [7]. In [8], the issue of optimal tradeoff between the average power and the average delay over memoryless block-fading channel has been addressed. Convexity and decreasing property of the optimal power/delay tradeoff curve for a finite buffer system have been established in [9] for Gaussian channel and independent identically distributed (i.i.d.) traffic. The effects of the transmission-delay requirement on the rate-adaptation schemes have been investigated from a theoretical point of view in [10], where perfect CSI knowledge at the transmitter is assumed and where achievable rates are evaluated under the assumption that error-free reception is available. The performance of selective-repeat automatic repeat request (ARQ) for adaptive modulation systems with selection transmit diversity is analyzed over a Nakagami- $m$  finite-state Markov channel (FSMC) in [11].

Reliability and throughput are two important aspects of packet-oriented communication systems over wireless channels. Hybrid ARQ that employs one code for error correction and another code for error detection is frequently used to simultaneously achieve these two goals. The coding rate of the forward-error-correction (FEC) codes is often adapted with channel conditions to cope with the random variations of the channel gain. Previous works ([12], [13], and the references therein) on adaptive hybrid ARQ investigate the error-correction code adaptation with the channel conditions, where the channel condition is estimated from the previous positive-acknowledgment (ACK)/negative-acknowledgment (NAK) feedbacks from the receiver in some *ad hoc* way. In [12], packet-error rate has been estimated using the count of NAK packets in different observation intervals for different modes of the adaptive scheme. Here, an adaptive error-control technique based on the use of type-I hybrid ARQ protocols is presented. The authors varied the coding rate of a family of Reed–Solomon codes, whereas the channel estimation is done using the ARQ protocol. In [13], stop and wait ARQ (SW-ARQ) is used to estimate the channels. According to the estimation results, the coding rate of Reed–Solomon codes is varied. XORing of the two consecutive erroneous copies is used to estimate the channel BER and to determine whether the mode change should be performed or not. All the previous works ([12], [13], and the references therein) neglected buffer queueing delay and packet-dropping probability. However, from the practical point of view, the queueing delay and the packet dropping should be considered for retransmission systems where packets are stored in a finite-sized buffer before transmission. In [14], joint effects of finite-length queueing, and adaptive modulation and coding for transmission over wireless links are analyzed. In [15], hybrid

ARQ systems with selective combining are investigated over a Rayleigh fading FSMC. The authors of this paper have studied several policy heuristic-based suboptimal algorithms for the solution of the partially observed MDP (POMDP)-formulated coding-rate-adaptation problem for type-I hybrid ARQ systems in [16].

We propose cross-layer optimization techniques to optimize the transmission power, the buffering delay, and the packet overflow rate for an adaptive type-I hybrid ARQ scheme. Both the transmission power and the transmission rate are varied with the buffer occupancy and the channel conditions to obtain the optimal scheduling strategy over correlated fading channels. In the first problem of this paper, we tackle the scheduling problem when both the perfect information of the channel and the observation feedback of the decoding results are available from the receiver. The transmitter takes a transmission decision based on the instantaneous channel state, and the SW-ARQ protocol is used to send decoding results of the transmission. It turns out that this cross-layer optimization problem can be solved using the tools provided by the theory of Markov decision process (MDP). In the second problem of this paper, we investigate the adaptation of the transmission power and rate for the case where the perfect CSI is not available, and the transmission decisions are taken based on the observation feedback of the previous transmissions. For this case, we propose a new technique to estimate the channel conditions. The control actions and the ACK/NAK feedbacks of several previous time slots are used as a history record to estimate the probability of ACK/NAK for the present time slot. We model the delay and the packet-overflow-constrained adaptive type-I hybrid ARQ as MDP. In essence, this is a POMDP problem. However, by truncating the history tracking and posing the problem as MDP, the computation of the optimal policies becomes much less computationally intensive. We analyze the performance of both models relying on the knowledge of the channel statistics, which is assumed to be modeled as the FSMC model. We consider both the correlated Rayleigh flat-fading channels [17] and the intersymbol-interference (ISI) channels [18]. To the best knowledge of the authors, the finite-state analysis of frequency-selective channel with the minimum-mean-square-error (MMSE) receiver has not previously been addressed. Furthermore, the optimal adaptation law is computed using the theory of MDP by applying relative value iteration, policy iteration, or linear-programming (LP) algorithms.

The organization of this paper is as follows. Section II introduces the general system model, the traffic model, and the channel model for the adaptive type-I hybrid ARQ scheme considered in this paper. In Section III, we demonstrate the formulations of joint power- and rate-adaptation problems as MDP. We discuss two cases of the problem according to the availability of perfect CSI through the feedback channel. We also provide the associated costs and transition matrices for both cases of CSI knowledge. The solution techniques employing iterative dynamic programming and LP are given in Section IV. Numerical results and discussions are given in Section V, and the conclusion is given in Section VI.

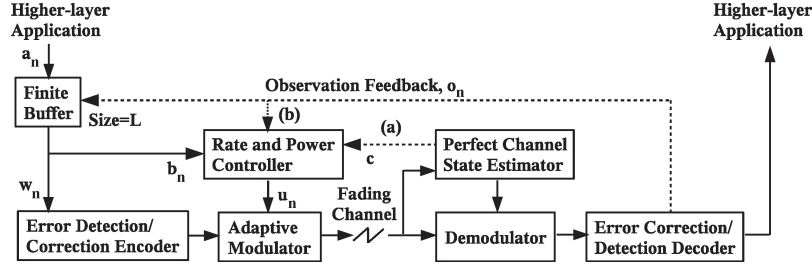


Fig. 1. Schematic of the adaptive type-I hybrid ARQ systems (a) when perfect CSI is available and (b) when perfect CSI is not available.

## II. GENERAL MODEL DESCRIPTION

Let us consider a point-to-point wireless link between two (possibly mobile) units equipped with a finite transmission buffer over a fading channel, as shown in Fig. 1. Packets are arriving from a higher layer application and are placed into a transmission buffer of length  $L$  packets. The size of each arriving packet is  $G$  bits. The time is slotted into a finite  $m$  number of slots (also called blocks),  $T_s$  denotes the duration of a typical time slot, and  $R_B = 1/T_s$  is the block transmission rate of the system. Therefore,  $n$ th time slot is the interval defined as  $[(n-1)T_s, nT_s]$ . In this paper, subscript  $n$  will always refer to a value of a particular variable at time slot  $n$ , and superscripts will always refer to a specific value of variable in a set.

### A. System Modeling

We assume that at the beginning of each time slot  $n$ , the transmitter takes  $w_n$  packets from the buffer and first encodes the corresponding  $k = w_n G$  bits using a high-rate error-detection code  $(k', k)$ . We use cyclic redundancy check (CRC) for error-detection purposes and assume that it is capable of detecting all the errors in the received codeword. The data packet with appended CRC is subsequently encoded using a FEC code. A particular  $(n', k')$  Bose–Chaudhuri–Hocquenghem (BCH) code (cf. [19]) is adopted in this paper for error correction. Note that the analysis is also general enough to take into account other codes, including convolutional codes, turbo codes, etc. The resulting codeword is modulated with an adaptive multilevel modulator and transmitted over the fading channel in time slot  $n$ . The modulation constellation and the transmission power are dependent on the action taken at the start of that particular time slot. The control action chosen at the start of a time slot is continued until the end of that time slot. We assume that all the packets transmitted in a block experience the same channel gain. Note that the processing unit at the data-link layer is a packet consisting of  $G$  bits and that the processing unit at the physical layer is a frame consisting of  $N_f$ -modulated symbols. We assume a Nyquist pulse-shaping filter with a bandwidth  $W = 1/T_{\text{sym}}$ , where  $T_{\text{sym}} = T_s/N_f$  is the symbol duration. Therefore, the number of symbols per frame can be expressed as  $N_f = N_c + (w_n G/R_d R_c R_i)$ , where  $N_c$  is the number of pilot and control symbols, and  $R_d = k/k'$  and  $R_c = k'/n'$  are the error-detection and error-correction coding rates, respectively.  $R_i = \log_2(M_i)$  is the number of bits that modulates a single transmitted symbol in the frame corresponding to the constellation  $M_i$  of the  $M_i$ -ary modulation scheme. The value

of  $w_n$  depends on the modulation and coding rates and can be given by  $w_n = ((N_f - N_c)R_i R_c R_d/G) = \text{constant} \times R_i$ . After being received at the receiver, the frame is demodulated. The error-correction decoder first attempts to correct any errors in the received demodulated frame, and then, the decoded frame is checked for error detection. Observation feedback is sent using the SW-ARQ protocol. If no errors are detected, the packets are delivered to the higher layer application, and an ACK observation feedback is sent to the transmitter. Accordingly, the transmitter removes those packets from the buffer. Otherwise, the receiver discards the packets and sends a NAK observation feedback requesting a retransmission of the same packets. The process is repeated until the packet is successfully received. We assume that the feedback channel is noiseless and that the observation feedback is received without any delay. Note that ACK and NAK are the observations in our framework and that we denote the observation state space by  $\mathcal{O} = \{O^1, O^2\} = \{\text{ACK}, \text{NAK}\}$ .

### B. Arrival Traffic Modeling and Buffer Dynamics

Let  $a_n$  denote the number of packets arriving at the buffer input in time slot  $n$ . It is assumed that all packets that arrive in time slot  $n$  can only be transmitted in time slot  $(n+1)$  or later. We assume that  $\{a_n\}$  is independent of the channel fading and noise processes. Let the state space of the input traffic be  $\mathcal{A} = \{A^0, A^1, \dots, A^Q\}$ , where  $A^k$  denotes the  $k$  packet arrival with probability  $p_a(A^k)$ . The steady-state expected arrival rate of the incoming packet can be given by  $\bar{A} = \mathbb{E}\{a_n\}$ . Let the transition probability of the incoming traffic from state  $A^i$  to  $A^j$  be denoted as  $p_a(A^j|A^i)$ , with  $\mathcal{P}_a$  being the incoming-packet transition probability matrix. Without loss of generality, we consider two special cases of incoming traffic: 1) uniformly distributed nonconstant traffic with  $p_a(A^k) = 1/(Q+1), \forall A^k \in \mathcal{A}$  and 2) Poisson-distributed bursty traffic with average arrival rate  $\bar{A}$ . The distribution of  $a_n$  for the Poisson traffic can be given as

$$p_a(a_n = A^k) = \exp(-\bar{A}T_s) \frac{(\bar{A}T_s)^k}{k!}, \quad k = 0, 1, \dots \quad (1)$$

The Poisson distribution is truncated such that the maximum number of incoming packets/slot  $Q$  is found by assuming that  $p_a(a_n = A^Q) \approx 0$  and by normalizing the distribution. We discretized the buffer in terms of incoming packet occupancy. Let  $\{B^0, B^1, \dots, B^L\}$  denote the state space of the buffer of length  $L$ , where  $B^k$  corresponds to the  $k$  packets in the

buffer. Therefore, the dynamics of the buffer in terms of packet occupancy is given by

$$b_{n+1} = \min \{b_n - o_n w_n + a_n, B^L\}. \quad (2)$$

The value of parameter  $o_n$  is equal to one if the previous transmission is successful and the ACK is received, and it is equal to zero if the previous transmission is unsuccessful and the NAK is received. It is clear that the transmitter has to send at most the number of packets that are currently stored in the buffer, i.e.,  $0 \leq w_n \leq L$ , even when the channel condition is good enough to send more packets. In addition, if the number of arriving packets is more than the empty space that the buffer currently has, additional packets will be dropped due to overflow.

### C. Markov Modeling of Rayleigh Fading Channel

The time-varying nature of the wireless channel poses a challenging task for the transmitter to reliably deliver packets to the receiver. Practical wireless channel has a memory, and therefore, the channel state at a particular time slot depends on the previous time slot. A slowly varying fading channel can be modeled as a correlated FSMC by partitioning instantaneous received fading power gain into finite number of states. This first-order Markov modeling has been widely used in the literature to capture the memory of the fading channels (see, e.g., [11], [15], and [20]–[22]). Let  $\{C^1 C^2 \dots C^K\}$  denote the state space of the channel with  $K$  states. We address both the flat-fading and frequency-selective fading channels. The occurrence of the flat fading or the frequency-selective fading depends on the system bandwidth and the coherence bandwidth of the channel. If the system bandwidth is larger than the coherence bandwidth, the channels undergo the frequency-selective fading channel [23].

Since flat fading is a special case of frequency-selective fading channel when the number of taps is one, we outline our notation and model for the frequency-selective fading case.<sup>1</sup> Let  $x_n$  be the sequence of signals sent by the transmitter with  $v = v_n = \mathbb{E}[x_n^2]$  denoting the transmitting power. We have assumed that the signaling is symmetric, i.e.,  $\mathbb{E}[x_n] = \bar{x}_n = 0$ . In time slot  $n$ , the channel with ISI can be approximated by an equivalent discrete-time linear filter. It has a finite-length impulse response of length  $M$  taps with coefficients  $g_n(0), \dots, g_n(M-1)$  that are assumed to be known to the receiver. For notational convenience, we introduce the received power gain as  $h_n(l) = g_n^2(l)$ ,  $l = 0, 1, \dots, M-1$ . In time slot  $n$ , the signal on the receiver side  $z_n$  is given by

$$z_n = \sum_{k=0}^{M-1} x_{n-k} g_n(k) + \omega_n \quad (3)$$

where  $\omega_n$  is the additive Gaussian noise with variance  $\sigma_\omega^2$ .

<sup>1</sup>The channel model that can be considered in this framework is not constrained only to the noninterference channels. In general, if the interference level from other users of the system at the receiver side can be modeled as a Markov chain, the received SNR for fixed transmission power can also be modeled as the Markov chain. Therefore, our framework can directly be applied by augmenting the channel state space to include the interference level from the other users. The computation of the optimal power and the rate control policy can be performed by using the MDP framework of this paper.

1) *Flat-Fading Case:* For the flat-fading case, the number of taps  $M$  is equal to one, and the channel is uniquely described by the sequence of fading power gains  $g_n = g_n(0)$ . We quantize the sequence of channel gains with the set of following received power gain thresholds  $\vec{\Gamma} = [\Gamma_0 \Gamma_1 \dots \Gamma_H]^T$ , where  $\Gamma_0 = 0$ ,  $\Gamma_H = \infty$ , and  $\Gamma_i < \Gamma_j$  for  $i < j$ . In the flat-fading case, the number of channel states  $K$  is equal to  $H$ . There are several methods to partition the received power gain. Without loss of generality, we use equal-probability method for our simulations due to the combination of its inherent simplicity and accuracy. In the equal-probability method,  $p_1 = p_2 = \dots = p_H$  [17], where

$$p_i = \int_{\Gamma_{i-1}}^{\Gamma_i} f_h(h) dh = F_h(\Gamma_i) - F_h(\Gamma_{i-1}) \quad (4)$$

is the steady-state probability of the  $i$ th,  $i = 1, 2, \dots, H$  power gain state of each tap. Functions  $f_h(h)$  and  $F_h(\Gamma)$  denote the probability density function (pdf) and the cumulative distribution function (cdf) of the received power gain  $h = h(0)$ . Rayleigh distribution is frequently used to describe the statistical time-varying nature of the received envelope of a flat-fading signal. The pdf of power gain  $h$  of such channel is exponentially distributed and can be written as

$$f_h(h) = \frac{1}{\bar{h}} \exp\left(-\frac{h}{\bar{h}}\right), \quad \text{for } h \geq 0 \quad (5)$$

where  $\bar{h} = \mathbb{E}\{h\}$  is the average power gain of the channel. The gain thresholds can be computed by combining (5) with (4) and numerically solving the resulting equations. The level crossing rate at threshold  $\Gamma_i$ ,  $i = 1, 2, \dots, H-1$  is given by

$$N_{\Gamma_i} = \sqrt{\frac{2\pi\Gamma_i}{\bar{h}}} f_m \exp\left(-\frac{\Gamma_i}{\bar{h}}\right) \quad (6)$$

where  $f_m = v_{ms}/\lambda_{rw}$  is the maximum Doppler frequency,  $v_{ms}$  is the speed of the mobile station, and  $\lambda_{rw}$  is the wavelength of the radio wave.

When the fading rate of the channel is slow, the channel states associated with the consecutive time slots are assumed to be the neighboring states. The crossover transition probabilities between gain states  $i$  and  $j$  can be written as [17]

$$p_c(j|i) = \frac{N_{\Gamma_j}}{p_i R_B} \quad \forall i=1, 2, \dots, H-1, \text{ and } j = i+1 \quad (7)$$

and

$$p_c(j|i) = \frac{N_{\Gamma_i}}{p_i R_B} \quad \forall i=2, 3, \dots, H, \text{ and } j = i-1. \quad (8)$$

Note that the self-transition probabilities can be computed using the fact that the sum of all outgoing transitions is equal to one. These probabilities are equal to the channel-state transition probabilities for the flat-fading channels. For a

flat-fading channel with power gain  $h$ , the received SNR  $\gamma$  can be calculated as

$$\gamma = \frac{vh}{\sigma_w^2}. \quad (9)$$

2) *Frequency-Selective Fading Case*: In the frequency-selective channel, power gains of all taps  $h_n(l) = g_n^2(l)$ ,  $l = 0, \dots, M-1$  are quantized using the  $H$  levels, as discussed in Section II-C1. Let  $\bar{h}(l)$  denote the average gain of tap  $l = 0, \dots, M-1$  of the frequency-selective channel. Therefore, the whole channel is characterized with  $K = H^M$  states, where each state  $C^k$  is characterized by the  $M$ -tuple  $k = [k_0, \dots, k_{M-1}]$  for each of the gain states of individual taps  $k_l = 1, 2, \dots, H$ ;  $l = 0, 1, \dots, M-1$ . Based on the experimental studies of [23], we assume that the channel gain in each tap is independent and follows the Rayleigh distribution. Therefore, the transition between the composite channel states  $C^k$ ,  $k = [k_0, \dots, k_{M-1}]$  and  $C^l$ ,  $l = [l_0, \dots, l_{M-1}]$  is given by

$$p_c(C^k|C^l) = \prod_{m=0}^{M-1} p_c(k_m|l_m). \quad (10)$$

We consider the use of the MMSE receiver to mitigate the ISI caused by frequency-selective channels [18]. The operation of the MMSE receiver is equivalent to filtering with a suitably chosen finite-impulse-response (FIR) filter. Let  $N_1$  and  $N_2$  denote the length of the noncausal and causal parts of the estimator. By using the sequence of the received symbols  $\mathbf{z}_n \triangleq [z_{n-N_2} z_{n-N_2+1} \dots z_{n+N_1}]$ , a linear estimate  $\hat{x}$  of the transmitted symbol  $x_n$  is given by

$$\hat{x}_n = \mathbf{a}_n^H \mathbf{z}_n \quad (11)$$

where  $\mathbf{a}_n$  is the coefficient of the estimator, and  $()^H$  is the Hermitian operator. If  $\mathbf{a}_n$  is allowed to vary with  $n$ , the MMSE solution can be given by

$$\mathbf{a}_n = \mathbf{Cov}(\mathbf{z}_n, \mathbf{z}_n)^{-1} \mathbf{Cov}(\mathbf{z}_n, x_n) \quad (12)$$

where  $\mathbb{E}(\cdot)$  is the expectation operator, and  $\mathbf{Cov}(x, y) \triangleq \mathbb{E}(xy^H) - \mathbb{E}(x)\mathbb{E}(y^H)$  is the covariance operator. The sequence of received symbols  $\mathbf{z}_n$  is given by

$$\mathbf{z}_n = \mathbf{H}\mathbf{x}_n + [\omega_{n-N_2} \omega_{n-N_2+1} \dots \omega_{n+N_1}]^T \quad (13)$$

where  $\mathbf{x}_n \triangleq [x_{n-N_2-M+1} x_{n-N_2-M+2} \dots x_{n+N_1}]^T$ , and  $\omega_n$  is the sequence of i.i.d. noise samples with variance  $\sigma_w^2$ .  $\mathbf{H}$  is the

$N \times (N + M - 1)$  channel convolution matrix [18] defined by (14), shown at the bottom of the page. The estimate  $\hat{x}$  can be expressed as

$$\hat{x}_n = \bar{x}_n + \mathbf{a}_n^H (\mathbf{z}_n - \bar{\mathbf{z}}_n) = \bar{x}_n + \sum_{k=-N_1}^{N_2} a_{n,k} \cdot (z_{n-k} - \bar{z}_{n-k}) \quad (15)$$

where  $\mathbf{a}_n = v_n \Sigma_n^{-1} \mathbf{s}$ . This equation is equivalent to filtering the difference  $z_n - \bar{z}_n$  with a linear filter with  $N = N_1 + N_2 + 1$  coefficients  $f_{n,k}$ ,  $k = -N_1, 1 - N_1, \dots, N_2$  given by

$$\mathbf{f}_n = [f_{n,N_2}^* f_{n,N_2-1}^* \dots f_{n,-N_1}^*]^T \triangleq \Sigma_n^{-1} \mathbf{s}. \quad (16)$$

Therefore, the estimate  $\hat{x}_n$  is given by

$$\hat{x}_n = \bar{x}_n + v_n \cdot \mathbf{f}_n^H (\mathbf{z}_n - \bar{\mathbf{z}}_n). \quad (17)$$

In the aforementioned equations,  $\bar{\mathbf{z}}_n$  and  $\Sigma_n$  are given by the following formula:

$$\bar{z}_n \triangleq \mathbb{E}(z_n) = \sum_{k=0}^{M-1} h_k \bar{x}_{n-k}$$

$$\bar{\mathbf{z}}_n \triangleq \mathbb{E}(\mathbf{z}_n) = [\bar{z}_{n-N_2} \bar{z}_{n-N_2+1} \dots \bar{z}_{n+N_1}]^T$$

$$\mathbf{V}_n \triangleq \mathbf{Cov}(\mathbf{x}_n, \mathbf{x}_n) = \text{diag}[v_{n-M-N_2+1}, \dots, v_{n+N_1}]$$

$$\mathbf{s} \triangleq \mathbf{H} [\mathbf{0}_{1 \times (N_2+M-1)} \mathbf{1}_{1 \times N_1}]^T$$

$$\Sigma_n \triangleq \mathbf{Cov}(\mathbf{z}_n, \mathbf{z}_n) = \sigma_w^2 \mathbf{I}_N + \mathbf{H} \mathbf{V}_n \mathbf{H}^H.$$

By using the similar approach as in [18] and [25], we approximate the output of the MMSE receiver with the Gaussian distribution.<sup>2</sup> This is a very useful approximation as we can calculate the BER using standard expressions for the additive Gaussian noise channels. Therefore, it is assumed that the pdf  $p(\hat{x}_n|x_n)$  is Gaussian, where the mean and the variance are given by

$$\mu_n = K_n \mathbf{f}_n^H \mathbf{s} x_n \quad (18)$$

$$\sigma_n^2 = K_n^2 \cdot (\mathbf{f}_n^H \mathbf{s} - v_n \mathbf{f}_n^H \mathbf{s} \mathbf{s}^H \mathbf{f}_n) \quad (19)$$

where  $K_n = (1 + (1 - v_n) \mathbf{f}_n^H \mathbf{s})^{-1}$ . Therefore, the SNR after the MMSE receiver is implicitly dependent on the power gains

<sup>2</sup>The merits and the accuracy of this approximation have previously been addressed by [24] for the MMSE multiuser receivers.

$$\mathbf{H} = \begin{pmatrix} g(M-1) & g(M-2) & \dots & g(0) & 0 & \dots & 0 \\ 0 & g(M-1) & g(M-2) & \dots & g(0) & \dots & 0 \\ & & & & \vdots & & \\ 0 & \dots & 0 & g(M-1) & g(M-2) & \dots & g(0) \end{pmatrix} \quad (14)$$

of individual taps  $h_n(0), \dots, h_n(M-1)$  and the transmission power  $v$ . This SNR can be expressed as

$$\begin{aligned} \gamma(h_n(0), h_n(1), \dots, h_n(M-1); v) &= \frac{\mu_n^2}{\sigma_{\omega, n}^2} \\ &= \frac{(\mathbf{f}_n^H \mathbf{s})^2}{\mathbf{f}_n^H \mathbf{s} - v_n \mathbf{f}_n^H \mathbf{s} \mathbf{s}^H \mathbf{f}_n} \end{aligned} \quad (20)$$

and this expression will be used to evaluate the packet-error probabilities of the adaptive type-I hybrid ARQ protocol.

### III. RATE AND POWER ADAPTIVE TRANSMISSION FOR TYPE-I HYBRID ARQ SYSTEMS

We consider the combined transmission-rate and power-adaptation technique for type-I hybrid ARQ systems over the correlated flat-fading channels as well as over the ISI channels. The heterogeneous traffics (e.g., voice, video, interactive messages, file transfers, web browsing, etc.) that are envisioned to support in the modern- and future-generation wireless networks have different QoS requirements. For example, each traffic type has its own delay requirements. In practice, the transmission buffers for wireless systems are of finite size. Due to the finite size of the buffer and the burstiness of the incoming traffic, packet overflows from the buffer are unavoidable over the wireless links. Likewise, the tolerance on the maximum packet overflow rate is dissimilar for different traffic types. Transmission power is another important factor for wireless devices that are usually operated with limited battery capacities. Therefore, wise minimization of transmission power is of paramount importance for wireless networks. In this section, we address the scheduling problems over wireless links that minimize the transmission power which is subject to the fact that both the packet delay in the buffer and the packet overflow rate from the buffer are less than some prescribed values. We adapt both the transmitter power and the modulation constellation with the instantaneous channel conditions and the instantaneous buffer occupancy. Thus, we are concerned with a system that can choose its modulation constellation among the discrete finite set of constellations  $\mathcal{M}$ . Let  $J$  be the total number of different constellations in the set and  $M_i, i = 1, \dots, J$  be the constellation size of a particular modulation scheme. In this paper, we consider only the discrete modulation classification since it has been observed in [2] that the maximum spectral efficiency of modulation is nearly the same under both the continuous and discrete rate adaptations.

We discuss two different cases for the problem at hand. In the first case, we assume that the perfect CSI is tracked at the receiver and sent to the transmitter without latency and errors. In this case, the scheduler adapts the transmission rate and power with the perfectly known channel state. Note that the buffer-state information is always known at the transmitter before transmission. Although the transmission decision is accurate when the perfect CSI is available at the transmitter, there is a

possibility of packet error depending on the state of the channel. This error can be known after decoding the received packet. We use the SW-ARQ protocol to notify the decoding result in terms of observation to the transmitter. The same feedback channel is used for both purposes.

Sometimes, in certain practical circumstances, the perfect CSI may not be available at the transmitter, and the transmission decision has to be based on the observations only. The second considered case deals with the transmission rate and power adaptation based on the buffer occupancy and the history of the observations and actions taken in the previous time slots. It is obvious that this case is suboptimal as compared with the optimal case when the perfect CSI is known.

#### A. When Both the Perfect CSI and Observations Are Known

We formulate the problem as average cost MDP that can be defined through the following ingredients: a set of time slots (also called decision epochs or stages)  $\mathcal{T} = \{1, 2, \dots, m\}$ , a finite set of system states  $\mathcal{S} = \{S^1, S^2, \dots, S^N\}$ , a finite set of actions  $\mathcal{U} = \{u^1, u^2, \dots, u^U\}$ , a set of state- and action-dependent immediate costs  $\mathcal{G} : \mathcal{K} \mapsto \mathbb{R}$ , and a set of state- and action-dependent transition probabilities  $\mathcal{P} : \mathcal{K} \mapsto \Pi(\mathcal{S})$ , where set  $\mathcal{K} = \{(s, u) : s \in \mathcal{S}, u \in \mathcal{U}\}$  is the set of state-action pairs,  $\mathbb{R}$  is the set of real numbers, and  $\Pi(\mathcal{S})$  is the set of discrete probability distributions over set  $\mathcal{S}$ .

The system state space for the perfect CSI case is composite and consists of buffer and channel states, namely,  $\mathcal{S} = \mathcal{B} \times \mathcal{C} = \{(B^0, C^1), (B^0, C^2), \dots, (B^L, C^{K-1}), (B^L, C^K)\}$  with a total number of states  $N = (L+1) \times K$ . The action state space maps to a set of transmission modes  $\mathcal{W}$ , which is composite and made up of discrete transmission power levels and discrete multilevel modulation schemes. The first action  $u^1$  corresponds to no transmission. The scheduler chooses this action when the buffer does not have enough packets to transmit or the channel condition is bad and the scheduler wants to save transmitter power, given that it can satisfy the constraint on the average delay and the average overflow rate. Other actions correspond to a particular power level and modulation scheme of the set of available transmission modes. Let  $\mathcal{W} = \{\text{TM}_1, \text{TM}_2, \text{TM}_3, \dots, \text{TM}_U\} = \{(0, 0), (P_{t_1}, R_1), (P_{t_1}, R_2), \dots, (P_{t_I}, R_{J-1}), (P_{t_I}, R_J)\}$  denote the set of transmission modes, where  $I$  is the total number of power levels, and  $U = IJ + 1$ . Let us denote the mapping between the action and transmission modes with function  $\Psi$ , i.e.,  $\Psi : \mathcal{U} \mapsto \mathcal{W}$ . The expressions for the costs and the transition probabilities are given in the following sections.

1) *Costs Related to the Objectives*: Our objective is to minimize three goals: long-term average transmitter power, long-term average delay, and long-term average packet overflow rate that can be given by

$$J_P = \lim_{m \rightarrow \infty} \frac{1}{m} \sum_{n=1}^m \mathbb{E} \{g_P(s_n, u_n)\} \quad (21)$$

$$J_D = \lim_{m \rightarrow \infty} \frac{1}{m} \sum_{n=1}^m \mathbb{E} \{g_D(s_n, u_n)\} \quad (22)$$

and

$$J_O = \lim_{m \rightarrow \infty} \frac{1}{m} \sum_{n=1}^m \mathbb{E} \{g_O(s_n, u_n)\} \quad (23)$$

where  $g_P(s_n, u_n)$ ,  $g_D(s_n, u_n)$ , and  $g_O(s_n, u_n)$  are the immediate power, the immediate packet delay in the buffer, and the immediate packet overflow costs from the buffer for state  $s_n$  and action  $u_n$ , respectively. These immediate costs are defined as follows.

**Power Cost:** The immediate power cost depends on the transmitter power level chosen. It can be noted that when the channel condition is bad, the transmission power can be raised to send packets. On the other hand, when the channel is in a higher state, the packet can be sent with the lowest transmitter power level. Therefore, the power cost is the transmitter power level chosen for a particular action  $u_n$  at a particular system state  $s_n$  and can be given by

$$g_P(s_n, u_n) = \Psi_1(u_n) \quad \forall s_n \in \mathcal{S} \quad (24)$$

where  $\Psi_1(u_n)$  indicates the first element of the transmission mode of action  $u_n$ . The power cost is independent of the current system state. However, it should be chosen according to the current system state (so that both the delay and the packet overflow-rate bounds are satisfied). Note that the current system state is dependent on the current channel state, the previous packet arrivals, and the previous channel state (hence, decoding results).

**Delay Cost:** The buffering delay experienced by a packet in the queue depends on the buffer occupancy and the average arrival rate. The delay is larger when the average buffer occupancy is higher or the arrival rate is smaller. The delay cost can be given from the well-known Little's law. The long-term average delay with this law can be stated in terms of the average buffer occupancy and the average arrival rate as

$$\bar{D} = \lim_{m \rightarrow \infty} \frac{1}{m} \sum_{n=1}^m \frac{\mathbb{E}\{b_n\}}{\bar{A}}. \quad (25)$$

Thus, we can express the immediate delay cost for state  $s_n = (b_n, c_n)$  and action  $u_n$  by the following formula:

$$g_D(s_n, u_n) = \frac{b_n}{\bar{A}} \quad \forall c_n \in \mathcal{C} \text{ and } u_n \in \mathcal{U}. \quad (26)$$

It can be noted that the delay cost is independent on the current channel state and action taken in the current time slot and only depends on the current buffer state. However, the current buffer state is determined by the decoding results of the previous time

slots (which is dependent on channel state) and the previous packet arrivals.

**Overflow Cost:** The buffer overflow occurs when the buffer has less vacancy than the number of incoming packets. The maximum number of packet arrivals is  $Q$ ; therefore, if the current buffer state is in  $\{B^{L-Q+1}, B^{L-Q+2}, \dots, B^L\}$ , there is a certain possibility of buffer overflow. For state  $s_n$  and action  $u_n$ , we can write the buffer overflow rate in packets/time slot by the following equation:

$$g_O(s_n, u_n) = \sum_{O^i \in \mathcal{O}} \sum_{a_j \in \mathcal{A}} \varphi(\psi(s_n) + a_j - O^i \Psi_2(u_n), B^L) \times p_a(a_j) p(O^i | \chi(s_n), u_n) \quad (27)$$

where function  $\varphi(x, y)$  returns the difference of  $x$  and  $y$  when  $x \geq y$  and 0 when  $x < y$ . Functions  $\chi(s_n)$  and  $\psi(s_n)$ , give the channel state  $c_n$  and the buffer state  $b_n$ , respectively, of the composite system state  $s_n$ ,  $\Psi_2(u_n)$  indicates the second element of the transmission mode for action  $u_n$  (i.e., the number of packets taken from the buffer  $w_n$ ), and  $p(o_n | \chi(s_n), u_n)$  is the probability of observation for the given channel state  $c_n = \chi(s_n)$  and action  $u_n$ .

Let the binary forward error-correction code  $(n', k')$  be capable of correcting  $t$  bit errors. Then, the NAK probability (frame-error probability) for channel state  $c_n$  and action  $u_n$  can be written as

$$p(O^2 | c_n, u_n) = \sum_{l=t+1}^{n'} \binom{n'}{l} (\tilde{P}_e(c_n, u_n))^l (1 - \tilde{P}_e(c_n, u_n))^{n'-l} \quad (28)$$

where  $\tilde{P}_e(c_n, u_n)$  is the average bit-error probability for channel state  $c_n$  and action  $u_n$ . Although any set of modulation schemes can be applied for our framework, without loss of generality, we consider the  $M$ -phase-shift-keying ( $M$ -PSK) modulation for the simulations. In the following, we present the BER expression for the frequency-selective channel only as the flat-fading channel is a special case of the frequency-selective channel when the number of taps in the channel filter model is one. There are two possible ways to determine the average bit-error probability. First, it can approximately be computed using the average received power gain  $\tilde{\gamma}(C^k)$  of the channel state  $C^k$  when action  $u^i$  is chosen [26] as

$$\tilde{P}_e(C^k, u^i) \approx \frac{1}{\Psi_2(u^i)} \operatorname{erfc} \left( \sqrt{\tilde{\gamma}(C^k, u^i)} \sin \left( \frac{\pi}{2\Psi_2(u^i)} \right) \right). \quad (29)$$

The average received power gain for state  $C^k \in \mathcal{C}$ ,  $k = [k_0, \dots, k_{M-1}]$  can be computed using (30), shown at the bottom of the page. Alternatively, the average bit-error

$$\tilde{\gamma}(C^k, u^i) = \frac{\int_{\Gamma_{k_0-1}}^{\Gamma_{k_0}} \dots \int_{\Gamma_{k_{M-1}-1}}^{\Gamma_{k_{M-1}}} \gamma(h_0, \dots, h_{M-1}; \Psi_1(u^i)) f_h(h_0) \dots f_h(h_{M-1}) dh_0 \dots dh_{M-1}}{\int_{\Gamma_{k_0-1}}^{\Gamma_{k_0}} \dots \int_{\Gamma_{k_{M-1}-1}}^{\Gamma_{k_{M-1}}} f_h(h_0) \dots f_h(h_{M-1}) dh_0 \dots dh_{M-1}} \quad (30)$$

probability for the  $M$ -PSK modulation corresponding to action  $u^i$  in the channel state  $C^k$  can be calculated as (31), shown at the bottom of the next page. The integrals in the aforementioned expressions can numerically be evaluated. If the number of quantization level is large, both of the aforementioned methods will give the same results.

2) *Transition Probability Matrix*: The transition probability for the considered type-I hybrid ARQ systems depends on the incoming traffic statistics, the current buffer occupancy, the feedback observations, and the channel statistics. It can be expressed by the following equation:

$$\begin{aligned} & p(s_{n+1}|s_n, u_n) \\ &= \sum_{O^i \in \mathcal{O}} \sum_{a_j \in \mathcal{A}} p_a(a_j) p_c(\chi(s_{n+1})|\chi(s_n)) p(O^i|\chi(s_n), u_n) \\ & \quad \times \delta(\psi(s_{n+1}) - \min((\psi(s_n) + a_j - O^i \Psi_2(u_n)), B^L)) \end{aligned} \quad (32)$$

where function  $\delta(x)$  returns one if  $x = 0$  and zero otherwise. Since no packet is transmitted for action  $u_1$ , the transition probability in that case does not depend on observation probability. For other actions, when the buffer does not have enough packets to transmit, the transition and cost matrices are corrected to avoid those actions.

### B. When Only Previous Observations Are Known

In this section, we present a general framework for the identification of the control law for the adaptive type-I hybrid ARQ system when the perfect knowledge of the CSI is not supplied to the transmitter. The transmitter in this case is supplied with the decoding results of previous transmissions in terms of the ACK/NAK feedback. We call the previous actions and their corresponding observations as the history. Since the channel state is only partially observable through the observations, the system state of the problem is also partially observable. The control of dynamic stochastic systems whose state cannot perfectly be observed falls under the theory of POMDP. It is known from [27] that the optimal control policies of the POMDP problems can be formulated as either complete-history-dependent or belief-state-dependent. Unfortunately, finding the optimal policies for all but the very simple examples is computationally intractable. Since the state space analyzed in this paper can be very large due to possible large buffer length, we resorted to finding an approximate control policy that is dependent only on the finite length of history tracking. Let  $H$  be the length of history that is being tracked and  $H_n = \{u_{n-1}, o_{n-1}, \dots, u_{n-H}, o_{n-H}\}$  be the history record at time slot  $n$ . Thus, the history state space denoted with  $\mathcal{H} = \{H^1, H^2, \dots, H^Z\}$  has a total of  $Z = (2 \times U)^H$  states. It is intuitively clear that by increasing the observation history to infinity, we can get the optimal policy for the problem at hand.

We also formulate the problem as an average cost MDP as in Section III-A. The system state space in this case is composed of the buffer and history states; therefore,  $\mathcal{S} = \mathcal{B} \times \mathcal{H} = \{(B^0, H^1), (B^0, H^2), \dots, (B^L, H^{Z-1}), (B^L, H^Z)\}$  with a total number of  $N = (L + 1) \times Z$  states. Our target is to minimize the average power, the average delay, and the average

overflow rate as given by (21)–(23), respectively. We use the same set of actions or, in other words, the same set of transmission modes as in Section III-A to also achieve the goals for this problem.

1) *Costs Related to the Objectives*: Since the power cost only depends on the action, whereas the delay cost only depends on the buffer state, these costs, therefore, are the same for both the fully observable and partially observable channel-state cases, which are given by (24) and (26), respectively.

The overflow occurs under the same buffer condition as in Section III-A1. The packet overflow rate from the buffer can be expressed as

$$\begin{aligned} g_{\mathcal{O}}(s_n, u_n) &= \sum_{O^i \in \mathcal{O}} \sum_{a_j \in \mathcal{A}} \varphi(\psi(s_n) + a_j - O^i \Psi_2(u_n), B^L) \\ & \quad \times p_a(a_j) p(O^i|\xi(s_n), u_n) \end{aligned} \quad (33)$$

where function  $\xi(s_n)$  returns the history state of the composite system state, and  $p(O^i|\xi(s_n), u_n)$  is the probability of observation  $O^i$  for the given history  $H_n = \xi(s_n)$  and action  $u_n$  at time slot  $n$ , which can be written as

$$\begin{aligned} & p(O^i|H_n, u_n) \\ &= P(O^i|u_{n-1}, o_{n-1}, \dots, u_{n-H}, o_{n-H}, u_n) \\ &= \frac{p(O^i, o_{n-1}, \dots, o_{n-H}|u_n, u_{n-1}, \dots, u_{n-H})}{p(o_{n-1}, o_{n-2}, \dots, o_{n-H}|u_{n-1}, u_{n-1}, \dots, u_{n-H})}. \end{aligned} \quad (34)$$

Conditional probabilities of the observation sequence, given the action sequence, can now be calculated by considering all the possible combinations for the states of underlying FSMC as

$$\begin{aligned} & p(o_n, o_{n-1}, \dots, o_{n-H}|u_n, u_{n-1}, \dots, u_{n-H}) \\ &= \sum_{c_n, \dots, c_{n-H}} p(c_n, \dots, c_{n-H}) \prod_{i=0}^H p(o_{n-i}|c_{n-i}, u_{n-i}) \end{aligned} \quad (35)$$

where  $p(c_n, \dots, c_{n-H})$  denotes the joint probability of all the channel states that the system occupies in the time slot from  $(n - H)$  to  $n$  and is given by

$$\begin{aligned} p(c_n, \dots, c_{n-H}) &= p_{c_{n-H}} \times p_c(c_{n-H+1}|c_{n-H}) \\ & \quad \times \dots \times p_c(c_n|c_n). \end{aligned} \quad (36)$$

In the aforementioned expression,  $p_{c_{n-H}}$  denotes the stationary probability of channel state  $c_{n-H} \in \mathcal{C}$ , and  $p_c(C^j|C^i)$ ,  $C^i = c_{n-H}, c_{n-H+1}, \dots, c_{n-1}$ ,  $C^j = c_{n-H+1}, c_{n-H+2}, \dots, c_n$  denotes the state transition probability given in Section II-C. Note that the calculation of expression  $P(o_n, o_{n-1}, \dots, o_{n-H}|u_n, u_{n-1}, \dots, u_{n-H})$  can also be done by performing the forward-backward method explained in [28]. This is due to the fact that the observation process  $o_n$  is, in fact, a hidden Markov process where the conditional probabilities of observation  $o_n$ , given the underlying FSMC state  $c_n$ , are also dependent on the current applied action  $u_n$ .

The choice of the separate buffer cost and the buffer overflow cost in the previously posed MDP deserves a more detailed explanation. First, it should be noted that buffer overflows can

always occur with nonzero probability in an ARQ system. This is due to the fact that even with the highest transmission power and the underlying channel being in the strongest state, there is a nonzero probability that an infinite succession of unsuccessful transmissions can occur. Second, the buffer overflow cost produces a different kind of transmission disruption compared to the transmission delay, and these costs cannot jointly be considered. The choice of maximum allowable delay and buffer overflow rate depends very much on the possible application. Data transmission can tolerate substantial delays, whereas buffer overflows (and packet losses) have to occur with negligible probability. As opposed to the data transmission, real-time video and audio transmission might not tolerate high transmission delays, whereas buffer overflows that would result in the loss of video or audio frames might be acceptable with some small probability.

2) *Transition Probability Matrix*: The transition probability for the partially observable channel-state case of type-I hybrid ARQ systems depends on the incoming traffic statistics, the current buffer occupancy, and the feedback observations. We can express it by the following equation:

$$\begin{aligned} & p(s_{n+1}|s_n, u_n) \\ &= \sum_{O^i \in \mathcal{O}} \sum_{a_j \in \mathcal{A}} p_a(a_j) p(O^i | \xi(s_n), u_n) \\ & \quad \times \delta(\psi(s_{n+1}) - \min((\psi(s_n) + a_j - O^i \Psi_2(u_n)), B^L)). \end{aligned} \quad (37)$$

Note that the same history is carried forward to the next time slot if no transmission action  $u_n$  is chosen in a particular time slot.

#### IV. SOLUTION TECHNIQUES FOR THE SCHEDULING PROBLEMS

For both cases, at each time slot  $n$ , suppose that the system occupies a state  $s_n = S^i$  and that the scheduler selects an action  $u_n$  from the set of actions  $\mathcal{U}_{S^i}$  available at state  $S^i \in \mathcal{S}$ , where  $\bigcup_{S^i \in \mathcal{S}} \mathcal{U}_{S^i} = \mathcal{U}$ . After an action  $u_n$  is selected, the system moves to the next state  $S^j \in \mathcal{S}$  according to the probability distribution  $p(s_{n+1} = S^j | s_n = S^i, u_n)$ , and the decision maker incurs a one-step immediate cost  $g(s_n, u_n)$ . The selection of an action  $u_n$  may depend on the current state, the current time, and the available information about the history of the system. A decision rule prescribes a procedure for action selection in each state at a particular time slot. Let  $\mu_n$  denote a decision rule at time slot  $n$ , then  $\mu_n : \mathcal{S} \mapsto \mathcal{U}_{\mathcal{S}}$ . A policy (also called control law)  $\pi$  specifies the decision rule to be used at all time slots, i.e.,

$\pi = \{\mu_1, \mu_2, \dots, \mu_m\}$ . Let  $\Pi$  denote the set of all admissible policies  $\pi$ . We assume that the policy does not vary with time slot  $n$ . A policy is called stationary if  $\mu_n = \mu, \forall n \in \mathcal{T}$  and has the form  $\pi = \{\mu, \mu, \dots, \mu\}$ ; for brevity, we denote it by  $\mu$ . The expected long-term average cost per stage with stationary policy  $\mu$  is

$$J_\mu = \lim_{m \rightarrow \infty} \frac{1}{m} \sum_{n=1}^m \mathbb{E}\{g(s_n, \mu(s_n))\}. \quad (38)$$

When the Markov chain induced by the policy  $\mu$  is ergodic, then we have  $J_\mu = \mathbb{E}\{g(s, \mu(s))\}$ . The policy  $\mu^*$  over the set of all stationary policies  $\Pi$ , which minimizes the average cost per stage (38), is called the optimal policy, and the corresponding optimal cost per stage is given by

$$J^* = \min_{\mu \in \Pi} J_\mu. \quad (39)$$

For a finite MDP, it is known that given any history-dependent policy, there exists a Markov policy, which is dependent only on the previous state, with the same average cost. Therefore, it is sufficient to restrict our attention to Markov policies while seeking the optimal policy [29]. For a nonconstant incoming traffic, in general, the formulated MDP is weakly communicating [10]. An MDP is said to be weakly communicating if there exists a closed set of states, in which each state is accessible from every other state in that set under some deterministic stationary policy, plus a possibly empty set of states which is transient under every policy. If the state spaces are finite, the costs are bounded, the system is stationary (i.e., the system equation, the cost per stage, and the transition probabilities do not change from one stage to the next stage), and the average cost per stage problem (39) can be solved using dynamic programming techniques.

##### A. Iterative Dynamic-Programming-Based Approach

It can be noted that if we want to minimize the transmitter power, the scheduler will send with a lower power level, and this, in turn, increases the delay and the overflows as the probability of success is reduced. Since the considered objectives are contradictory, in this paper, we would like to investigate the tradeoff between these objectives. The problem with conflicting objectives can be solved in two ways, namely, forming the problem as an unconstrained MDP (UMDP) or as a constrained MDP (CMDP). In UMDP, we find the total immediate cost by summing the weighted combination of the different immediate costs [i.e.,  $g(s_n, \mu(s_n)) = \beta_P g_P(s_n, \mu(s_n)) + \beta_D g_D(s_n, \mu(s_n)) + \beta_O g_O(s_n, \mu(s_n))$ ], where  $\beta_1$  and  $\beta_2$  are

$$\tilde{P}_{e, \mathbf{M}\text{-PSK}}(C^k, u^i) = \frac{\int_{\Gamma_{k_0-1}}^{\Gamma_{k_0}} \dots \int_{\Gamma_{k_{M-1}-1}}^{\Gamma_{k_{M-1}}} \operatorname{erfc}\left(\sqrt{\gamma(h_0, \dots, h_{M-1}; \Psi_1(u^i))} \sin\left(\frac{\pi}{2\Psi_2(u^i)}\right)\right) f_h(h_0) \dots f_h(h_{M-1}) dh_0 \dots dh_{M-1}}{\Psi_2(u^i) \int_{\Gamma_{k_0-1}}^{\Gamma_{k_0}} \dots \int_{\Gamma_{k_{M-1}-1}}^{\Gamma_{k_{M-1}}} f_h(h_0) \dots f_h(h_{M-1}) dh_0 \dots dh_{M-1}} \quad (31)$$

nonnegative constants] and formulate the problem as an average cost per stage problem as in (38). The optimal policy  $\mu^*$  of such a weakly communicating UMDP can be computed using any iterative dynamic-programming technique, such as relative value or the policy iteration algorithm, for a particular fixed value of constants  $\beta_1$  and  $\beta_2$  [30].

### B. LP-Based Approach

In CMDP, one objective cost is minimized while keeping the other objective costs (also called the constrained costs) below some given bounds. In the proposed framework, our objective is to minimize the average power cost, imposing certain upper bounds on the average delay cost and the average overflow rate cost. Mathematically, the stationary policy which satisfies the following constrained optimization problem is our optimal policy  $\mu^*$

$$\min_{\mu^* \in \Pi_R} J_{\mu^*,P}, \text{ subject to: } J_{\mu^*,D} \leq \tilde{D} \text{ and } J_{\mu^*,O} \leq \tilde{O}F \quad (40)$$

where  $J_{\mu^*,P}$ ,  $J_{\mu^*,D}$ , and  $J_{\mu^*,O}$  are the optimal average power, the average delay, and the average overflow-rate costs, respectively, for optimal policy  $\mu^*$  over the set of stationary randomized policy  $\Pi_R$ . The nonnegative constants  $\tilde{D}$  and  $\tilde{O}F$  are the maximum allowable average delay in time slots and the average overflow rate in packets/time slot, respectively. The values of these two bounds depend on the application being considered. The CMDP problem previously formulated can be solved using the equivalent LP methodology described in [29]. It can be shown that there is a one-to-one correspondence between the feasible (and optimal) solution of the LP and the feasible (and optimal) solution of the CMDP. LP is feasible if and only if CMDP is feasible [31]. Let  $\nu(s, u)$  represent the “steady-state” probability that the process is in state  $s$  and the action  $u$  is applied. We seek to calculate the control policy which is represented in terms of probability distribution  $\nu$  over  $\mathcal{S} \times \mathcal{U}$ . The optimal policy  $\nu^*$  can be obtained by solving the linear program

$$\text{minimize } \sum_{s \in \mathcal{S}, u \in \mathcal{U}} g_P(s, u) \nu(s, u) \quad (41)$$

$$\text{subject to } \sum_{s \in \mathcal{S}, u \in \mathcal{U}} g_D(s, u) \nu(s, u) \leq \tilde{D} \quad (42)$$

$$\sum_{s \in \mathcal{S}, u \in \mathcal{U}} g_O(s, u) \nu(s, u) \leq \tilde{O}F \quad (43)$$

$$\sum_{u \in \mathcal{U}} \nu(t, u) = \sum_{s \in \mathcal{S}, u \in \mathcal{U}} \nu(s, u) p(t|s, u) \quad (44)$$

$$\sum_{s \in \mathcal{S}, u \in \mathcal{U}} \nu(s, u) = 1 \quad (45)$$

$$\nu(s, u) \geq 0 \quad \forall s \in \mathcal{S} \text{ and } \forall u \in \mathcal{U} \quad (46)$$

where  $t \in \mathcal{S}$ . The inequality constraints in (42) and (43) are posed to keep the long-term average delay and the average overflow rate below the specified bounds, whereas the equality constraint in (44) satisfies the well-known Chapman–Kolmogorov

equation. The constraint in (45) guarantees that the sum of the probabilities  $\nu(s, u)$  is equal to one, whereas (46) confirms the nonnegativity of the individual probabilities. Suppose that there exists an optimal solution  $\nu^*$  to the LP problem. Then, there exists a stationary policy  $\mu^*$  that is optimal for the CMDP problem. The optimal policy  $\mu^*$  for CMDP is randomized and is uniquely characterized with probability  $\theta_{\mu^*(s)}(u)$  of applying policy  $u \in \mathcal{U}$  in state  $s \in \mathcal{S}$ , where

$$\theta_{\mu^*(s)}(u) = \frac{\nu^*(s, u)}{\sum_{u' \in \mathcal{U}} \nu^*(s, u')}, \quad \text{if } \sum_{u' \in \mathcal{U}} \nu^*(s, u') > 0. \quad (47)$$

If  $\sum_{u' \in \mathcal{U}} \nu^*(s, u') = 0$  for some  $s \in \mathcal{S}$ , an action that drives the system to  $\mathcal{S}_{\nu^*} = \{s \in \mathcal{S} : \sum_{u' \in \mathcal{U}} \nu^*(s, u') > 0\}$  is chosen in each state [29]. The aforementioned linear program can easily be solved using interior-point methods [32]. By using the standard software optimization packages such as Matlab, the linear program with  $10^4$  variables can easily be solved.

## V. NUMERICAL RESULTS

We present the numerical results to explore the performance of different schemes and system parameters introduced in Section II. We explore the adaptive type-I hybrid ARQ systems over both the flat-fading and frequency-selective channels in this section. The cost associated with particular objective is described in Section III. The objective of this section is to illustrate the qualitative behavior of the proposed scheduling framework. It is the authors' intention to show the relative performance of average power and average overflow rate with respect to the average delay for different values of Doppler frequencies, buffer sizes, incoming traffic rates, and frequency selectivities of the channel.

We also show the comparison of two considered cases, namely, when the perfect CSI is available and when it is not available. Unless specified otherwise, we use the following data for all the numerical simulations: maximum Doppler frequency  $f_m = 200$  Hz, number of channel states  $K = 4$  (as in [17]), number of blocks per second  $R_B = 10^4$ , noise power  $\sigma^2 = 1$  mW, average received power gain  $g_0 = 1$  dB for each tap [2], available transmitter power levels  $P_{t_1} = 20$  mW,  $P_{t_2} = 50$  mW, Q-PSK and eight-PSK modulation schemes, buffer size  $L = 50$  packets, Poisson-distributed traffic with maximum packet arrivals  $Q = 7$  packets and average packet arrival  $\bar{A} = 1$  packet, incoming packet size  $G = 255$  bits, and frame size  $N_f = 255$  symbols. The bits used for error detection and control symbols are not counted for throughout the calculations ( $N_c = 0$ ). FEC is used only in Fig. 5. From the aforementioned data, it is clear that the number of action is  $U = 5$ . In the aforementioned example, the dimensionality of the state space is  $50 \times 4 = 200$  for the perfect CSI case, and the computation of the optimal policy using either relative value iteration or LP is easily performed.

The data rate in bits per second depends on three parameters: number of blocks per second  $R_B$ , incoming packet rate  $\bar{A}$  in packets per time slot, and number of bits per packet  $G$ . Therefore, the data rate can be given by  $R_B \bar{A} G$ . For the aforementioned parameters, the data rate is  $10^4 \times 1 \times 255 = 2.55$  Mb/s.

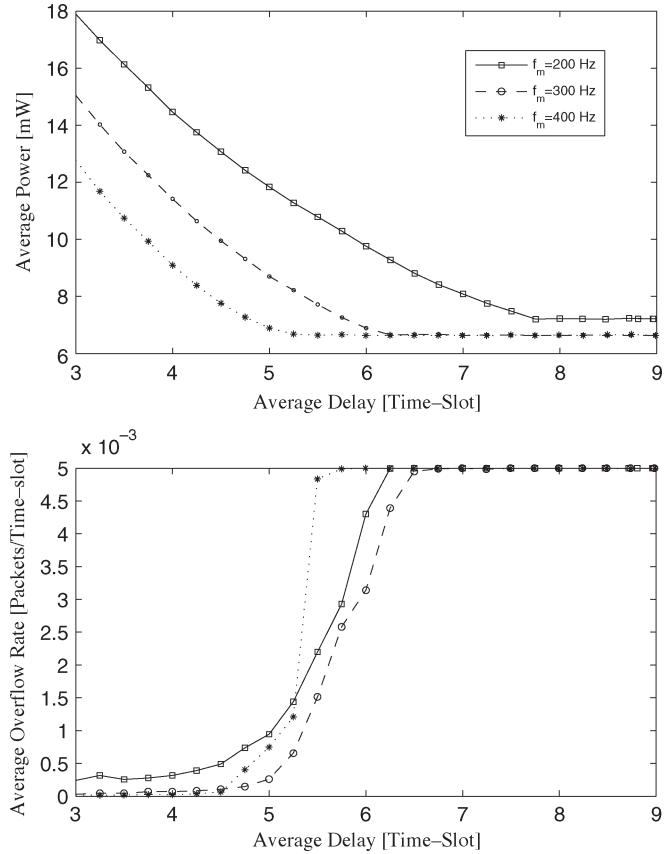


Fig. 2. Effect of Doppler frequency  $f_m$  on the average power versus average delay and the average overflow rate versus average delay for the flat-fading channels.

The optimal policies and costs are computed using the following steps: 1) Compute transition probability matrices  $\mathcal{P}$  using (32) and cost matrices  $\mathcal{G}$  using (24), (26), and (27); 2) compute the optimal probability distribution  $\nu^*$  by solving the linear program given by (41)–(46); 3) calculate the optimal policy for all states using (47); and 4) compute optimal power, delay, and overflow-rate costs by substituting the value of  $\nu^*$  into (41)–(43).

*Observation 1—Study of Fading Rate on the Average Power and Packet Overflow Over Flat-Fading Channels When Perfect CSI Is Known:* We show the dependence of the average power and the average packet overflow rate for three values of maximum Doppler frequency, namely,  $f_m = 200, 300,$  and  $400$  Hz in Fig. 2. In order to demonstrate the effects of the overflow-rate bound, we have chosen  $\bar{O}F = 5 \times 10^{-3}$  packets/time slot for this example. The uniformly distributed packet arrival with  $Q = 2$  is assumed in this case. It is seen from the figure that the average power decreases as the average delay increases. Furthermore, for the same average delay, the average power is less for higher Doppler frequencies (and higher fading rates). This fact can be explained as follows: With the increase of fading rate, the likelihood of getting higher channel state after lower channel state increases. In order to save power, the optimal scheduler has a strategy to store packets in the buffer at lower channel states and to send those in the higher channel states with lower power. However, in order to meet a specified delay requirement for a particular application, in slower fading

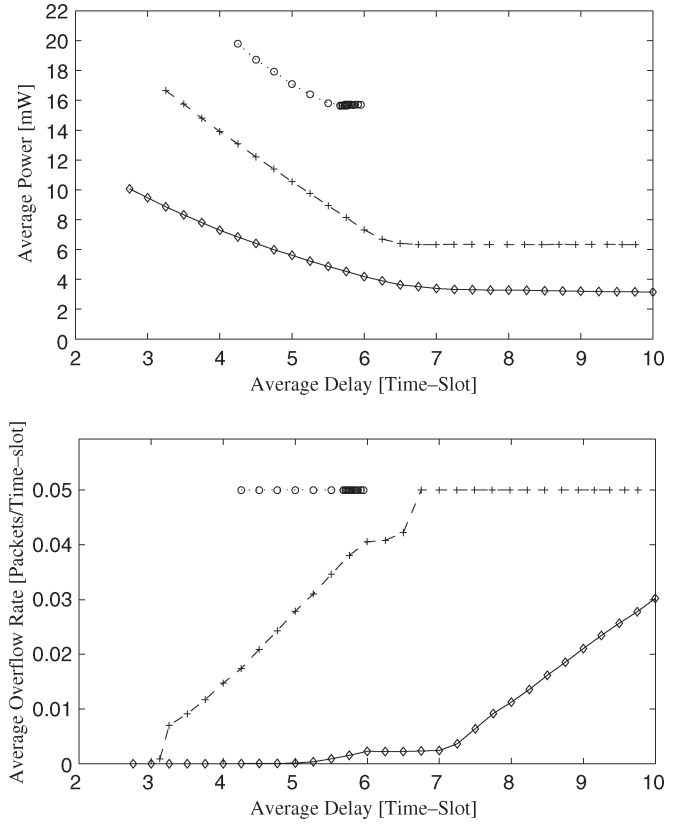


Fig. 3. Effect of arrival packet rate  $\bar{A}$  on the average power versus average delay and the average overflow rate versus average delay for flat-fading channels. Solid, dashed, and dotted curves correspond to the average arrival rate  $\bar{A} = 0.5, 1.0,$  and  $1.5,$  respectively.

channels, the scheduler is forced to send packets even in lower channel states with higher transmission power action. As a result of this phenomenon, the average power for the same delay requirement increases when the fading rate decreases. The simulation results show that the packet overflow rate does not vary significantly with the fading rate.

*Observation 2—Study of Packet Arrival Rate on the Average Power and Packet Overflow Over Flat-Fading Channels When Perfect CSI Is Known:* Fig. 3 shows the effect of different packet arrival rates on the average power versus average delay and the average packet overflow rate versus average delay curves. The overflow-rate bound for this observation has been chosen to be  $\bar{O}F = 5 \times 10^{-2}$  packets/time slot. The scheduler needs more power when the average arrival rate increases. With the increase of packet arrival rate, the scheduler gets less idle time (the time when the scheduler has nothing to send). Therefore, the scheduler needs to send packets even in weaker channel states to be able to maintain the delay requirements. As the chance of full buffer is lower when the average arrival rate is lower, the packet overflow rate, therefore, is also less for lower arrival rate.

Note that for larger incoming packet rates of  $\bar{A} = 1.5$  packet/s, the overflow-rate bound (43) with the average overflow rate of  $\bar{O}F = 5 \times 10^{-2}$  packets/time slot is attained for all feasible delays  $\bar{D}$ . This is due to the fact that the buffer of length  $L = 50$  packets is too short to cope with very high incoming packet rates, rendering overflows inevitable.

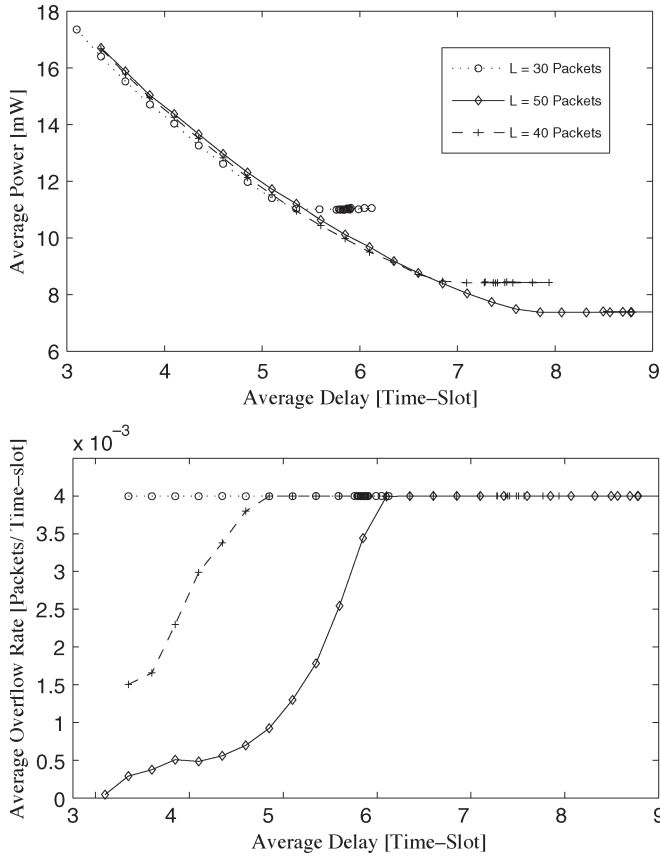


Fig. 4. Effect of buffer size  $L$  on the average power versus average delay and the average overflow rate versus average delay for the flat-fading channels.

*Observation 3—Study of Buffer Size on the Average Power and Packet Overflow Over Flat-Fading Channels When Perfect CSI Is Known:* In Fig. 4, we show the power/delay tradeoff and overflow rate versus the delay curves for different buffer sizes  $L$ . The plots show that as the buffer size decreases, the minimum achievable power increases, and the feasible delay region also decreases. In the low delay region, the power is almost the same for all considered buffer sizes  $L = 30, 40,$  and  $50$  packets. This is due to the nonutilization of the whole buffer under more stringent delay requirement. The power is slightly less for smaller buffer due to the increased packet overflow rate. In the higher delay region, while the packet overflow rate attains the bound of  $\bar{O}F = 4 \times 10^{-3}$  packets/time slot, the power is increased for smaller buffer sizes. This is due to the fact that when the buffer size is larger, the scheduler has increased flexibility to store more packets in the lower channel state and to send those with lower power in the higher channel state. Therefore, to maintain the same delay, the scheduler has to use higher power as the buffer size decreases.

*Observation 4—Study of the Influence of Channel Coding on the Power Performance of ARQ Scheme:* Channel coding is used to increase the error resilience of data bits sent over a noisy channel by adding the redundancy in the codewords. We have explored the use of (255, 215) binary BCH code that corrects up to five bit errors to protect packets sent over the time-varying flat-fading channel [19]. To ensure a fair comparison to the case without coding, it is assumed that the bandwidth of the system is constant, making the code symbol rate in the coding

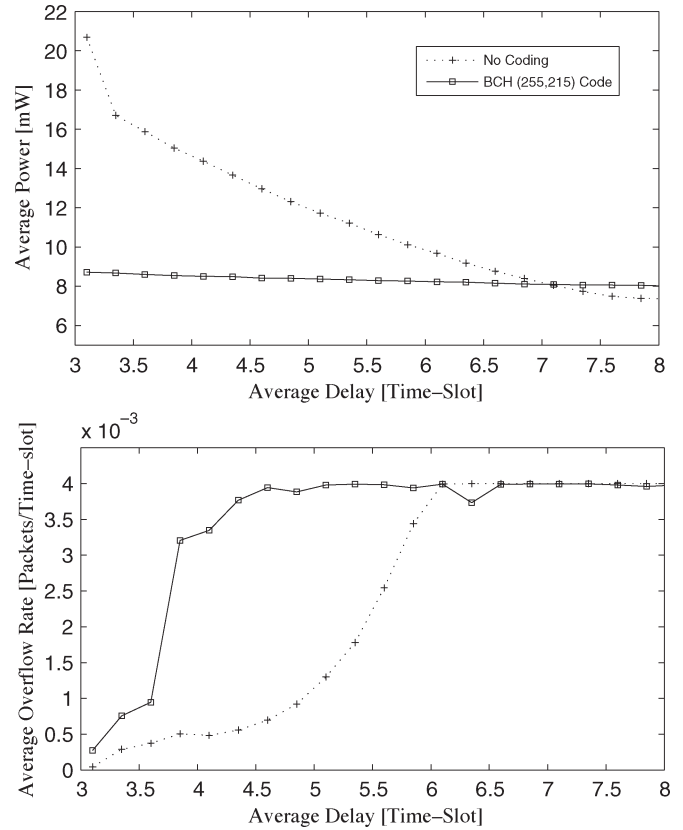


Fig. 5. Influence of channel coding on the power performance of the optimal scheduler in the perfect CSI flat-fading channel.

case equal to the bit rate in the no-coding case. Therefore, by employing the aforementioned code, each packet contains only 215 b instead of 255 in the no-coding case. Furthermore, to ensure the fair comparison between the two cases, in the coding case, we have increased the average number of incoming packets and the buffer occupancy by the factor of  $255/215$  to keep the average incoming traffic in bits and the buffer capacity in bits constant. Fig. 5 shows the comparison of the power versus the delay performance of the hybrid ARQ system with and without coding. The buffer overflow rate is constrained to  $\bar{O}F = 4 \times 10^{-2}$  packets/slot, the buffer capacity is equal to  $255 * 50$  b, and the Doppler frequency is equal to 200 Hz. It can be seen that for the lower values of the delay, the use of coding substantially reduces the operating average power of the optimal scheduler. However, for the case of very large delays, the no-coding case needs slightly lower powers than the coding case. As a result of adding the redundancy in the coding case, less information is contained in each packet, and less data can be sent during the longer intervals of favorable channel conditions. This is of particular importance under less stringent delay requirements. For the simulation settings previously outlined, it has been observed that the packet success rate is very high for the higher channel states even without the use of coding, making the use of coding for higher channel states unnecessary.

*Observation 5—Study of the Influence of Frequency-Selective Fading on the Power Performance of ARQ Scheme:* Fig. 6 shows the comparison of the average power and the

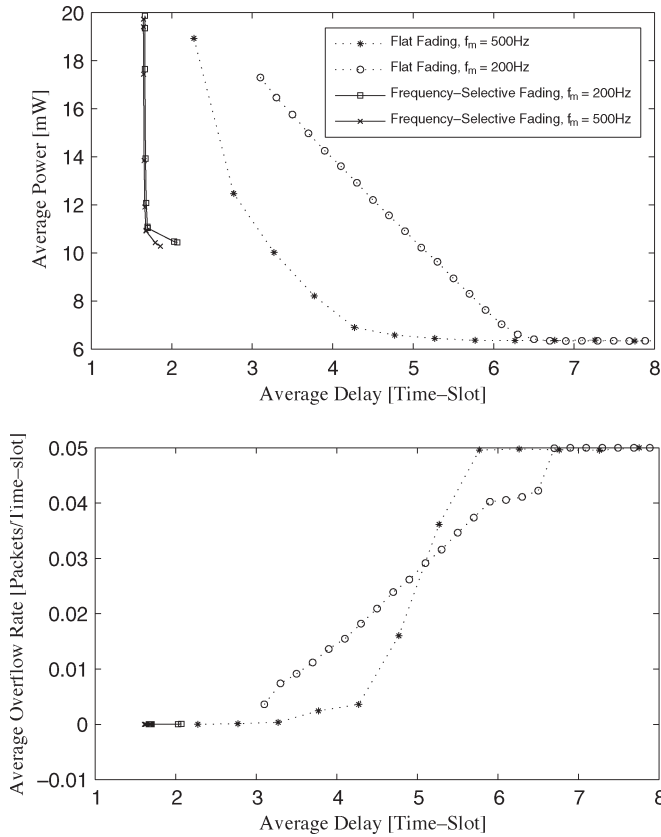


Fig. 6. Influence of the channel model on the power performance of the optimal scheduler in the perfect CSI flat-fading and frequency-selective fading channels.

average overflow-rate performance in terms of the delay for the flat-fading and frequency-selective fading channels. The buffer capacity is assumed to be 255 packets, the buffer overflow rate is constrained to  $\bar{O}F = 5 \times 10^{-2}$  packets/slot, and the frequency-selective channel is modeled as an FIR filter with  $M = 2$  taps. Each tap of that frequency-selective channel is assumed to follow the Rayleigh distribution. Total received energy is assumed to be constant to ensure the fair comparison between the flat-fading and frequency-selective channels. Therefore, the average gain for the flat-fading case is  $\bar{h} = 10$ , whereas the average gain for the frequency-selective case is  $\bar{h}(0) = \bar{h}(1) = 5$  for each of the taps of the FIR filter describing the frequency-selective channel.

It can be seen that due to combining the two discernible paths of the frequency-selective channel performed by the MMSE receiver, delays achieved by the optimal scheduler are significantly less than the flat-fading channel. Note that the equivalent channel gain after the MMSE combining receiver has fewer time variations than the channel gains of each of the taps of the frequency-selective channel prior to MMSE combining. This implies that the scheduler does not need to utilize the buffer (as much as in the flat-fading case) and increase the delay in order to schedule transmission in higher channel states.

*Observation 6—Comparison of the Power Performance of Hybrid ARQ Schemes With History Tracking and Perfect CSI:* Knowledge of CSI enables the scheduler to suitably adapt the

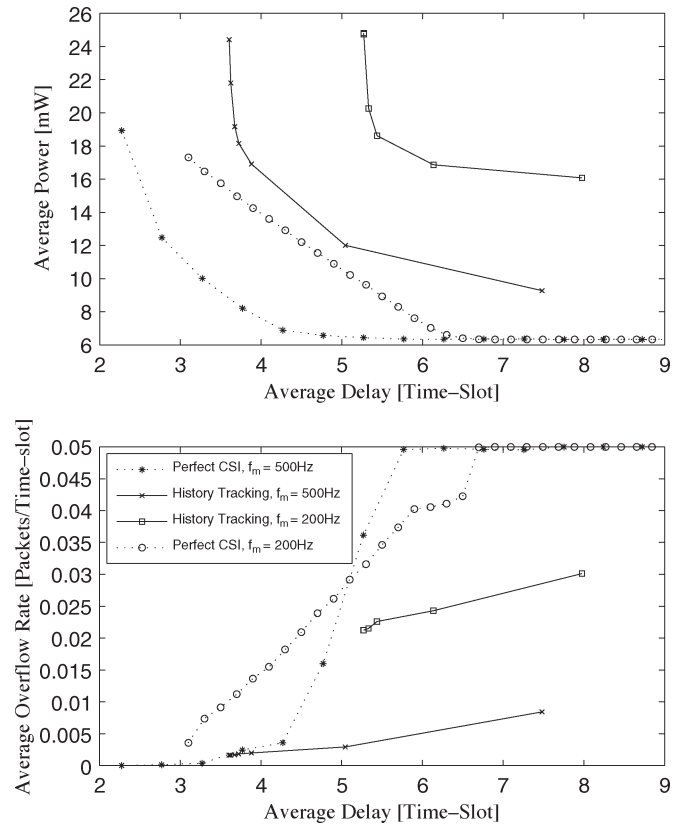


Fig. 7. Influence of the perfect and nonperfect CSIs on the power performance of the optimal scheduler in the flat-fading channel.

transmitted power and the transmission rate to the time-varying channel conditions. When the CSI is not perfectly known, such as the case of history tracking presented in Section III-B, the scheduler has to act more cautiously considering that it is not certain of precise channel state. Fig. 7 shows the increase (compared to the perfectly known CSI) in the needed average transmission power for the case of CSI provided by the history tracking. It is assumed that the scheduler tracks the channel based only on the previous observation (ACK/NAK) and the previous action taken, i.e., history length of  $H = 1$ . In order to demonstrate the effects of the overflow-rate bound, we have chosen  $\bar{O}F = 5 \times 10^{-2}$ . Note that the optimal history-dependent policy is computed by solving the MDP problem, as described in Section III-B. The long-term average power, the average delay, and the average overflow rate costs for both the perfect CSI case and the history-tracking case are computed using (21)–(23) of Section III-A.

As expected, it can be observed in Fig. 7 that the power needed for the transmission with the history tracking is larger than in the case of knowledge of the perfect CSI. With the increase of fading rate  $f_m$ , average powers for the same delay in both the perfect and imperfect CSI cases decrease. While that phenomenon has been explained for the perfect CSI case in Observation 1, the case of history tracking deserves additional explanations. Two effects influence the power performance of the history-tracking algorithm with the increase of fading rate: 1) increase of the diversity provided by the more frequent

changes in the channel states (as discussed in Observations 1) and 2) decrease of ability to predict the outcome of the next transmission due to more frequent changes in the channel. The two effects have the opposite influence on the power performance, and it can be seen that for the simulation settings in Fig. 7, the first effect is dominant, facilitating the decrease of the needed power with the increase of Doppler frequency.

## VI. CONCLUSION

This paper presents a general approach for the optimal delay and the packet-overflow-constrained adaptive joint power and rate allocation for the type-I hybrid ARQ systems. The presented optimal adaptation laws can be obtained through a control-theoretic framework of MDPs. We have discussed the adaptation strategy for two cases: when the perfect knowledge of the CSI is provided by the estimator at the receiver and when no perfect knowledge of the CSI is known and the channel state is estimated by the history-tracking mechanism.

For both problems, the state spaces, the control actions, the transition probabilities, and the cost functions of the respective MDPs have been identified in this paper. We have suggested two algorithmic approaches to effectively solve such MDPs, namely, relative value iteration, policy iteration, and LP algorithms.

We have explored the influence of the channel model (in terms of frequency selectivity) on the power performance for the optimal scheduling schemes. The transmitter power can be reduced by increasing the transmission delay. In addition, the power decreases with the increase of fading rate, the increase of buffer size, and the decrease of average arrival rate. It has been seen that due to the increased diversity provided by the MMSE filter receiver for frequency-selective channels, the variation of the SNR at the output of the filter is decreased. This results in the decreased delay for the same power as compared to the flat-fading case. We have also investigated the case when the perfect CSI is not available at the transmitter at the time of transmission and compared the results with that of the perfect CSI case. The power allocation based on the history-tracking results in an increase in average power as compared to the perfectly observed case. It has been seen through the simulations that the packet scheduling for the hybrid ARQ scheme with no perfect CSI works better as the fading rate decreases.

## REFERENCES

- [1] S. Nanda, K. Balachandran, and S. Kumar, "Adaptation techniques in wireless packet data services," *IEEE Commun. Mag.*, vol. 38, no. 1, pp. 54–64, Jan. 2000.
- [2] S. T. Chung and A. J. Goldsmith, "Degrees of freedom in adaptive modulation: A unified view," *IEEE Trans. Commun.*, vol. 49, no. 9, pp. 1561–1571, Sep. 2001.
- [3] A. J. Goldsmith and P. P. Varaiya, "Capacity of fading channels with channel side information," *IEEE Trans. Inf. Theory*, vol. 43, no. 6, pp. 1986–1992, Nov. 1997.
- [4] A. J. Goldsmith and S.-G. Chua, "Variable-rate variable-power MQAM for fading channels," *IEEE Trans. Commun.*, vol. 45, no. 10, pp. 1218–1230, Oct. 1997.
- [5] R. A. Berry and E. M. Yeh, "Fundamental performance limits for wireless fading channels—Cross-layer wireless resource allocation," *IEEE Signal Process. Mag.*, vol. 21, no. 5, pp. 59–68, Sep. 2004.
- [6] B. Collins and R. Cruz, "Transmission policy for time varying channel with average delay constraints," in *Proc. Allerton Conf. Commun., Control, Comput.*, Monticello, IL, Sep. 1999, pp. 709–717.
- [7] E. Uysal-Biyikoglu, A. E. Gamal, and B. Prabhakar, "Energy-efficient packet transmission over a wireless link," *IEEE/ACM Trans. Netw.*, vol. 10, no. 4, pp. 487–499, Aug. 2002.
- [8] R. A. Berry and R. G. Gallager, "Communication over fading channels with delay constraints," *IEEE Trans. Inf. Theory*, vol. 48, no. 5, pp. 1135–1149, May 2002.
- [9] D. Rajan, A. Sabharwal, and B. Aazhang, "Delay-bounded packet scheduling of bursty traffic over wireless channels," *IEEE Trans. Inf. Theory*, vol. 50, no. 1, pp. 125–144, Jan. 2004.
- [10] A. K. Karmokar, D. V. Djonin, and V. K. Bhargava, "Optimal and suboptimal packet scheduling over correlated time varying flat fading channels," *IEEE Trans. Wireless Commun.*, vol. 5, no. 2, pp. 446–457, Feb. 2006.
- [11] G. Femenias, "SR ARQ for adaptive modulation systems combined with selection transmit diversity," *IEEE Trans. Commun.*, vol. 53, no. 6, pp. 998–1006, Jun. 2005.
- [12] M. Rice and S. B. Wicker, "Adaptive error control over slowly varying channels," *IEEE Trans. Commun.*, vol. 42, no. 2–4, pp. 917–926, Feb.–Apr. 1994.
- [13] H. Minn, M. Zeng, and V. K. Bhargava, "An ARQ scheme with adaptive error control," *IEEE Trans. Veh. Technol.*, vol. 50, no. 6, pp. 1426–1436, Nov. 2001.
- [14] Q. Liu, S. Zhou, and G. B. Giannakis, "Queuing with adaptive modulation and coding over wireless links: Cross-layer analysis and design," *IEEE Trans. Wireless Commun.*, vol. 4, no. 3, pp. 1142–1153, May 2005.
- [15] Q. Zhang and S. A. Kassam, "Hybrid ARQ with selective combining for fading channels," *IEEE J. Sel. Areas Commun.*, vol. 17, no. 5, pp. 867–880, May 1999.
- [16] A. K. Karmokar, D. V. Djonin, and V. K. Bhargava, "POMDP-based coding rate adaptation for type-I hybrid ARQ systems over fading channels with memory," *IEEE Trans. Wireless Commun.*, vol. 5, no. 12, pp. 3512–3523, Dec. 2006.
- [17] H. S. Wang and N. Moayeri, "Finite-state Markov channel—A useful model for radio communication channels," *IEEE Trans. Veh. Technol.*, vol. 44, no. 1, pp. 163–171, Feb. 1995.
- [18] M. Tüchler, A. C. Singer, and R. Koetter, "Minimum mean squared error equalization using a priori information," *IEEE Trans. Signal Process.*, vol. 50, no. 3, pp. 673–683, Mar. 2002.
- [19] S. B. Wicker, *Error Control Systems for Digital Communication and Storage*. Englewood Cliffs, NJ: Prentice-Hall, 1995.
- [20] C.-D. Iskander and P. T. Mathiopoulos, "Fast simulation of diversity Nakagami fading channels using finite-state Markov models," *IEEE Trans. Broadcast.*, vol. 49, no. 3, pp. 269–277, Sep. 2003.
- [21] A. Chockalingam, M. Zorzi, L. B. Milstein, and P. Venkataram, "Performance of a wireless access protocol on correlated Rayleigh-fading channels with capture," *IEEE Trans. Commun.*, vol. 46, no. 5, pp. 644–655, May 1998.
- [22] Q. Zhang and S. A. Kassam, "Finite-state Markov model for Rayleigh fading channels," *IEEE Trans. Commun.*, vol. 47, no. 11, pp. 1688–1692, Nov. 1999.
- [23] T. S. Rappaport, *Wireless Communications: Principles and Practice*, 2nd ed. Englewood Cliffs, NJ: Prentice-Hall, 2002.
- [24] H. V. Poor and S. Verdú, "Probability of error in MMSE multiuser detection," *IEEE Trans. Inf. Theory*, vol. 43, no. 3, pp. 858–871, May 1997.
- [25] H. V. Poor and X. Wang, "Iterative (turbo) soft interference cancellation and decoding for coded CDMA," *IEEE Trans. Commun.*, vol. 47, no. 7, pp. 1046–1061, Jul. 1999.
- [26] J. G. Proakis, *Digital Communications*, 4th ed. New York: McGraw-Hill, 2000.
- [27] S. Russel and P. Norvig, *Artificial Intelligence: A Modern Approach*, 2nd ed. Englewood Cliffs, NJ: Prentice-Hall, 2003.
- [28] L. R. Rabiner, "A tutorial on hidden Markov models and selected applications in speech recognition," *Proc. IEEE*, vol. 77, no. 2, pp. 257–286, Feb. 1989.
- [29] M. L. Puterman, *Markov Decision Processes: Discrete Stochastic Dynamic Programming*. New York: Wiley, 1994.
- [30] D. P. Bertsekas, *Dynamic Programming and Optimal Control*, 2nd ed, vol. II. Belmont, MA: Athena Scientific, 2001.
- [31] E. Altman, *Constrained Markov Decision Processes: Stochastic Modeling*. London, U.K.: Chapman & Hall, 1999.
- [32] S. Boyd and L. Vandenberghe, *Convex Optimization*. Cambridge, U.K.: Cambridge Univ. Press, 2004.



**Dejan V. Djonin** received the B.Sc. and M.Sc. degrees from the University of Belgrade, Belgrade, Serbia, in 1996 and 1999, respectively, and the Ph.D. degree from the University of Victoria, Victoria, BC, Canada, in 2003.

From 1998 to 2000, he was with the Department of Telecommunications, Institute Mihajlo Pupin, Belgrade, where he worked on the development of an antenna array processing system. In 2005 and 2006, he held a Natural Sciences and Engineering Research Council of Canada Postdoctoral Fellowship at the

Department of Electrical and Computer Engineering, University of British Columbia, Vancouver, BC. He is currently with the Dyaptive Inc., Vancouver. His research interests include applications of control theory in multimedia communication systems, wireless communications, information theory, and machine learning.

Dr. Djonin served as an Assistant Program Chair of the Wireless Communications and Networking Conference 2004 and as a Technical Program Committee Member of ICC 2005 and Globecom 2003. In 2002, he received the Outstanding Paper Award for Young Researchers at the International Symposium on Information Theory and Its Applications.

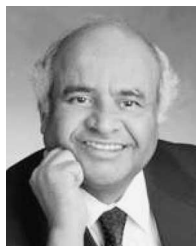


**Ashok K. Karmokar** (S'04) received the B.Sc. and M.Sc. degrees in electrical and electronic engineering from the Bangladesh University of Engineering and Technology (BUET), Dhaka, Bangladesh, in 1998 and 2002, respectively. He is currently working toward the Ph.D. degree in electrical and computer engineering with the Department of Electrical and Computer Engineering, University of British Columbia, Vancouver, BC, Canada.

From 1998 to 2002, he was with the Bangladesh University of Engineering and Technology, where he

served as a Lecturer and, then, as an Assistant Professor with the Department of Electrical and Electronic Engineering. His current research interests include resource allocations, stochastic packet scheduling, and applications of artificial intelligence algorithms in wireless multimedia networks.

Mr. Karmokar was the recipient of the Patrick David Campbell Graduate Fellowship, the Ann and William Messenger Graduate Fellowship, the University Graduate Fellowship, and the Ph.D. Tuition Fee Award from the University of British Columbia. He was also the recipient of the Dean's List Award, the University Merit Scholarship, the Altaf Hossain Fellowship, and the Dr. Rashid Memorial Scholarship from BUET, the Excellence Recruitment Award from the University of Victoria, and the Werner Von Siemens Excellence Award from Siemens AG.



**Vijay K. Bhargava** (S'70-M'74-SM'82-F'92) received the B.Sc., M.Sc., and Ph.D. degrees from Queen's University, Kingston, ON, Canada, in 1970, 1972, and 1974, respectively.

He was with the University of Victoria, Victoria, BC, Canada, from 1984 to 2003 and with Concordia University, Montreal, QC, Canada, from 1976 to 1984. Currently, he is a Professor and Head of the Department of Electrical and Computer Engineering, University of British Columbia, Vancouver. He is the coauthor of the book *Digital Communications*

*by Satellite* (Wiley, 1981), the coeditor of *Reed-Solomon Codes and Their Applications* (IEEE, 1994), and the coeditor of *Communications, Information and Network Security* (Kluwer, 2003). His research interest is wireless communications.

Dr. Bhargava is a Fellow of the Engineering Institute of Canada, the Canadian Academy of Engineering, and the Royal Society of Canada. He was nominated by the IEEE Board of Directors for the Office of IEEE President-Elect. He has served on the Board of the IEEE Information Theory Society and the IEEE Communications Society. He was the Former President of the IEEE Information Theory Society. He is an Editor of the IEEE TRANSACTIONS ON WIRELESS COMMUNICATIONS. He was the recipient of the IEEE Centennial Medal in 1984, the IEEE Canada's McNaughton Gold Medal in 1995, the IEEE Haraden Pratt Award in 1999, the IEEE Third Millennium Medal in 2000, the IEEE Graduate Teaching Award in 2002, and the Eadie Medal of the Royal Society of Canada in 2004.